Calculation of dopant segregation ratios at semiconductor interfaces

Chihak Ahn[1] and Scott T. Dunham[1,2]
[1]*Department of Physics, University of Washington, Seattle, Washington 98195, USA*
[2]*Department of Electrical Engineering, University of Washington, Seattle, Washington 98195, USA*
(Received 29 August 2007; published 4 November 2008)

We analyzed dopant segregation at semiconductor interfaces by equilibrating chemical potentials of dopants and electrons on each side of the interface. We apply the theory to Si/strained-SiGe interfaces and compare the predictions with existing experimental data. The calculations include changes in effective density of states (with particular attention to high-temperature hole effective mass), band-gap narrowing due to composition and temperature, and lattice parameter changes. We find that strong B segregation is dominated by stress effects, while moderate P or As segregation is dominated by changes in electronic band structure. We also observe that calculated stress energy is nearly temperature independent.

DOI: 10.1103/PhysRevB.78.195303 PACS number(s): 73.20.At, 73.90.+f

The effort to make semiconductor devices smaller and faster has had great success during the last 40 years. As a result, a single transistor has become smaller than 100 nm. In fabricating such small devices, controlling dopant concentration and diffusion is a critical issue, and surfaces and interfaces play an important role in dopant redistribution. Strong surface or interface effects also make nanoscale material properties distinct from conventional bulk properties.

Dopant segregation is an important interface phenomena and has been investigated both theoretically[1–4] and experimentally.[5–8] However, previous theoretical works lack accuracy or are limited to special cases. In Ref. 2, the electron energy appears to have been calculated in an inconsistent way. A more recent study by Boguslawski *et al.*[4] was limited to an extreme case where the dopant concentration is at the solubility limit because they assumed a dopant reservoir contacting the substrate. In our previous analysis,[3] B segregation was explained based only on strain compensation. In this work, we investigate the segregation ratio at semiconductor interfaces, leading to corrections to previous analyses by Hu.[1,2] We then apply this analysis to give quantitative predictions for Si/SiGe systems.

Dopant segregation occurs until the chemical potential μ reaches the same value on both sides of interface. Using Si/SiGe as an example, the segregation ratio k_{seg} is given as a solution of

$$\mu(k_{\text{seg}}N)_{\text{Si}_{1-x}\text{Ge}_x} = \mu(N)_{\text{Si}}, \tag{1}$$

where N is a dopant concentration on the Si side of interface. Hu[1,2] separated the chemical potential into parts: atomic and electronic. In the atomic part, dopant atoms were introduced into Si or SiGe with charge carriers at intrinsic Fermi level. However, the defect level (donor or acceptor level) E_d is a more proper level to introduce charge carriers and is consistent with subtracting ionized fraction of dopant in electronic step as done by Hu.[1,2] Low-temperature behavior further supports this, as some of the charges remain at defect level (not at intrinsic Fermi level).

The total free energy of N dopant atoms in SiGe is given by

$$G = Nu - V_0 N \Delta\vec{\epsilon} \cdot \mathbf{C} \cdot \vec{\epsilon}(N_{\text{Ge}}) - T\Delta S, \tag{2}$$

where Nu is the total internal energy of dopants, V_0 is a lattice site volume of relaxed $\text{Si}_{1-x}\text{Ge}_x$, $\mathbf{C}$ is the elastic stiffness tensor of $\text{Si}_{1-x}\text{Ge}_x$, $\Delta\vec{\epsilon}$ is the normalized induced strain due to dopant,[9] $\vec{\epsilon}(N_{\text{Ge}})$ is the applied strain, and ΔS is the change in entropy due to doping. The internal energy is

$$Nu = -fNZe\psi + N\bar{E}^b + (1-f)NE_d + (n-n_i)E_c - (p-n_i)E_v, \tag{3}$$

where f is the ionized fraction of dopant, Z is the charge state of dopant, $n(p)$ is the electron (hole) concentration, and n_i is the intrinsic carrier concentration. In Eq. (3), the first term is the electrical potential energy of ion, the second term is the averaged binding energy of dopant-Ge pairs over the total number of dopants, and the last three terms are electron energies. Averaged binding energy rather than direct binding energy[10] should be used since pairing probability is less than 1. Stress energy [the second term in Eq. (2)] is the reduced form of general tensor equation under normal stress conditions ($\theta\beta\beta_{\text{Ge}}NN_{\text{Ge}}$ in Refs. 1, 2, and 5). For simplicity, we will describe it as NE^s.

The entropy term is

$$\Delta S = k \ \ln\frac{\Omega_a(N)}{\Omega_a(0)}\frac{\Omega_e(N)}{\Omega_e(0)}, \tag{4}$$

where $\Omega_a(\Omega_e)$ is the number of possible configurations of atoms (electrons) due to dopant. Detailed calculations of Ω_a and Ω_e can be found in Ref. 2, but in counting the number of possible atomic configuration in Eq. (4), we added the assumption that B can replace only Si and not Ge, which is supported by highly suppressed BI complex formation with Ge.[11] Conversely, P or As diffusivity in strained $\text{Si}_{1-x}\text{Ge}_x$ is slightly higher than in Si,[12,13] which implies that dopants can replace Ge sites without restriction. To include this factor, we define $\tilde{Z}=(1-Z)/2$. If charge neutrality ($n-p-ZfN=0$) and full ionization ($f=1$) are assumed within Maxwell-Boltzmann statistics, then

$$nE_c - pE_v + kT \ln \Omega_e^{\text{Total}}(N) = NE_F. \tag{5}$$

Thus Eq. (2) is simplified to

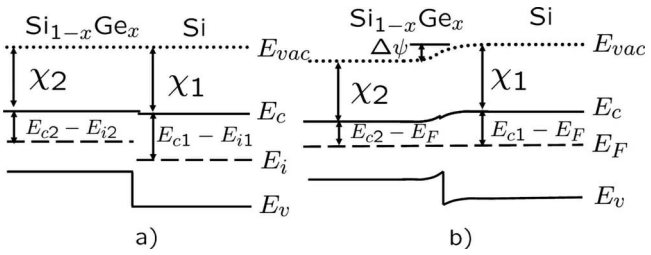

FIG. 1. Band alignment at strained-$Si_{1-x}Ge_x$/Si interface (a) without band bending and (b) with band bending. Charge neutrality breaks down near the junction due to different work functions. This builds up an electric potential and causes band bending across the junction.

$$G = N\left(-Ze\psi + ZE_F + \bar{E}^b + E^s + kT\ln\frac{N}{N_L - \tilde{Z}N_{\mathrm{Ge}}}\right), \quad (6)$$

where N_L is the lattice site concentration. Finally, the electrochemical potential of a dopant is given as a derivative of G with respect to N,

$$\mu = -Ze\psi + ZE_F + \bar{E}^b + E^s + kT\ln\frac{N}{N_L - \tilde{Z}N_{\mathrm{Ge}}}. \quad (7)$$

Selecting reference energy is important in using Eq. (7) in Eq. (1). Although Hu *et al.*[5] and Moriya *et al.*[7] used zero-field $Si_{1-x}Ge_x$/Si heterostructure band alignment, charge redistribution shifts $Si_{1-x}Ge_x$ band to equalize Fermi levels in both regions within a few Debye lengths $\sqrt{\epsilon_{\mathrm{Si}}kT/q^2N}$. Near the interface, charge neutrality does not hold, and thus, Eq. (5) is not valid. However, the Debye length is only on the order of 1 nm at 900 °C and 5×10^{19} cm^{-3}, which is the experimental condition in the works of Hu *et al.*[5] and Moriya *et al.*[7] Thus Fig. 1(b) is the proper band alignment, and Eqs. (1) and (7) can be combined to yield the segregation ratio

$$k_{\mathrm{seg}} = (1 - \tilde{Z}x)\exp[(Ze\Delta\psi - \Delta\bar{E}^b - \Delta E^s)/kT], \quad (8)$$

where x is the Ge fraction. Δ indicates the difference between regions 2 and 1 throughout this paper (with exception of $\Delta\epsilon$). The built-in potential term $e\Delta\psi$ (the work-function difference) is also a function of k_{seg}, and it is given by

$$e\Delta\psi = \Delta\chi + \Delta(E_c - E_F) = \Delta\chi + kT\ln\frac{N_{c2}}{n_2}\frac{n_1}{N_{c1}}, \quad (9)$$

where $\Delta\chi$ is the difference in electron affinities and subscript 1 (2) denotes the Si ($Si_{1-x}Ge_x$) region.

We used the numerical solution of Eq. (8) to compare our calculations with experiments. However, the two limiting cases determined by the ratio between the dopant concentration and intrinsic carrier density provide a guide for the range of segregation ratio. Under intrinsic condition $n=n_i=\sqrt{N_cN_v}\exp(-E_g/kT)$, and the intrinsic segregation ratio is given as

TABLE I. Induced strain due to dopants and associated volume expansion coefficient $\beta(\Delta\epsilon=\beta N_L)$. The values in parentheses are experimental data.

	P	As	B
$\Delta\epsilon$	−0.08	0.018	−0.302
$\beta(1\times10^{-24}\ \mathrm{cm}^3)$	−1.6(−1.9 [a])	0.36 (−0.4 [b])	−6.04(−6.3 [c])

[a]Reference 24.
[b]Reference 23.
[c]Reference 25.

$$k_{\mathrm{seg}} = (1 - \tilde{Z}x)\left(\frac{N_{c2}N_{v1}}{N_{c1}N_{v2}}\right)^{Z/2}\exp[(Z\Delta\chi - \Delta\bar{E}^b - \Delta E^s + Z\Delta E_g/2)/kT]. \quad (10)$$

Under extrinsic conditions, n_1/n_2 becomes $1/k_{\mathrm{seg}}$ for n type or $k_{\mathrm{seg}}[N_{c1}N_{v1}/(N_{c2}N_{v2})]\exp(\Delta E_g/kT)$ for p type ($n_i^2=np$). Applying these results in Eq. (8) yields the extrinsic segregation ratio

$$k_{\mathrm{seg}} = \sqrt{(1 - \tilde{Z}x)\frac{N_{c2,v2}}{N_{c1,v1}}}\exp[(Z\Delta\chi - \Delta\bar{E}^b - \Delta E^s - \tilde{Z}\Delta E_g)/2kT]. \quad (11)$$

For p-type material, N_v replaces N_c in Eq. (11). Note that $\tilde{Z}\Delta E_g$ is used instead of $Z\Delta E_g$ in an extrinsic case.

The three major factors in segregation ratio [Eqs. (10) and (11)] are changes in effective density of states (EDS), bandgap narrowing, and stress energy. (i) EDS: as more Ge is incorporated, EDS decreases because Ge-induced strain removes degeneracy of band structure. When compressive biaxial stress is applied, the electron EDS at room temperature rapidly decreases to 2/3 of unstressed value since compressive biaxial stress lowers energy of four conduction-band minima out of six. We calculated high-temperature N_{c2} value based on Eq. 22 and Table I in Ref. 14. Since electron density-of-states mass is almost constant with varying Ge fraction[15] and temperature,[16] this is a good approximation. Hole EDS varies in a more complicated way due to nonparabolicity of bands. Since no hole EDS data have been reported at high temperature, we calculated high-temperature hole EDS by integrating density-of-states effective mass provided by Fu *et al.*[17] As shown in Fig. 2, the change in electron EDS is much less than that in hole EDS. This difference causes B (P and As) to segregate out of (into) strained SiGe under intrinsic doping conditions [Eq. (10)]. Under extrinsic conditions, changes in EDS lead both types of dopants to segregate out of strained SiGe, but the effect is weaker for donors due to slowly varying electron EDS.

(ii) ΔE_g: there are many experimental measurements of strained- $Si_{1-x}Ge_x$ band gap as summarized by Yang *et al.*[14] When $x<0.40$, the deviation among the data is small and Yang *et al.* suggested $-0.896x+0.396x^2$ for ΔE_g,[14] which was used in our segregation calculations. Since the band structure of strained SiGe is similar to that of Si and has similar temperature dependence,[14] ΔE_g is temperature independent for $x<0.4$. The electric field due to the reduced

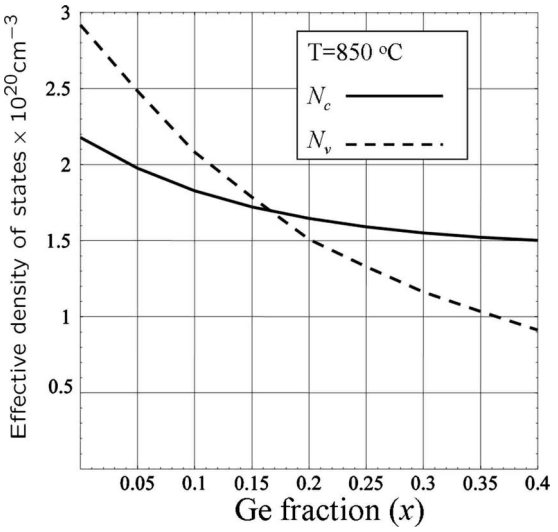

FIG. 2. Effective density of states in $Si_{1-x}Ge_x$. Biaxial compressive stress reduces sixfold degeneracy of conduction-band minima to fourfold degeneracy; thus, electron EDS of $Si_{1-x}Ge_x$ approaches 2/3 of that pure Si as Ge content increases. However, hole EDS decreases continually as more Ge is added.

band gap of $Si_{1-x}Ge_x$ results in the opposite type of intrinsic segregation for donors and acceptors, and it has the strongest effect on intrinsic donor segregation into Si. However, the band-gap difference has a minimal impact on extrinsic donor segregation due to aligned conduction band. For acceptors, a large built-in potential arises since band alignment occurs at the valence-band maximum. This causes B segregation into $Si_{1-x}Ge_x$.

(iii) ΔE^s: the stress energy was calculated by considering temperature and Ge dependence of lattice and elastic constants. Assuming pseudomorphic growth conditions, the applied strain in biaxially stressed $Si_{1-x}Ge_x$ is given by

$$\epsilon_{\parallel}(x,T) = \frac{a(0,T) - a(x,T)}{a(x,T)}, \quad \epsilon_{\perp}(x,T) = \nu\epsilon_{\parallel}(x,T), \quad (12)$$

where $\epsilon_{\parallel}(\epsilon_{\perp})$ is the in-(out-of-) plane strain and ν is the Poisson ratio $(-2C_{12}/C_{11})$. The lattice constant $a(x,T)=a_0(x)[1+\int_{298}^{T}\alpha(x,T')dT']$, where $\alpha(x,T)$ is the linear-expansion coefficient and was taken from Ref. 18. The room-temperature lattice constants $a_0(x)$ were obtained from Ref. 19. Combining the temperature dependence of Si elastic constants[20] with the Ge concentration dependence,[19] we estimated elastic constants $C_{11}(x,T)$ and $C_{12}(x,T)$ as

$$C_{11}(x,T) = (165.8 - 37.3x - 0.0128T) \text{ GPa}, \quad (13)$$

$$C_{12}(x,T) = (63.9 - 15.6x - 0.00480T) \text{ GPa}. \quad (14)$$

The induced strain $\Delta\vec{\epsilon}$ is defined as a shift in relaxed lattice constant of doped Si and can be extracted from energy vs lattice-constant curve.[9] Energy was calculated for a 64 atom supercell using the density-functional theory (DFT) code VASP.[21] We used PW91 generalized gradient approximation (GGA) potential[22] with 2^3 k-point and relatively high-energy cutoff of 340 eV for B and 250 eV for P and As. Induced

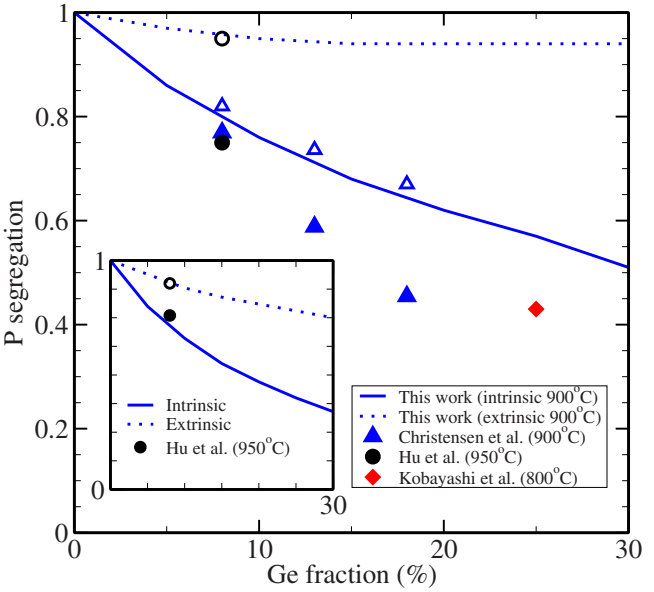

FIG. 3. (Color online) P segregation ratio at strained-$Si_{1-x}Ge_x$/Si interface. Filled symbols represent experimental values and open symbols represent corresponding theoretical values. The predicted value for Kobayashi *et al.* (Ref. 35) is not given because their experimental conditions were beyond the Maxwell-Boltzmann regime. Inset shows As segregation ratio at 950 °C.

strain due to B and P agrees well with experimental data, but for As, the calculation shows an opposite sign to the experimental value by Cargill *et al.*[23] (Table I). However, the absolute difference is small and discrepancy could be explained by the existence of As-vacancy complexes.[26] Unlike the two factors above, strain compensation is dependent not on the type of dopant but on the size of dopant. Consequently, it is the largest factor for the small B atom due to a large negative-induced strain (Table I), and it causes B to segregate into the Ge-rich region. On the other hand, strain compensation is much weaker for P and As, and electric-field effects overwhelm stress effects and result in segregation into Si.

In the segregation equations, there are two minor factors: the binding energy E^b and the electron affinity $\Delta\chi$. The binding energy E_b was also calculated using DFT. For all three cases (i.e., B-Ge, P-Ge, and As-Ge) the magnitude of direct binding energy was less than a couple tens of meV, and thus, averaged binding energy can be ignored in our calculations. $\Delta\chi$ is equal to $-\Delta E_c$ at low temperature as seen in Fig. 1(a). While theoretical calculations using $\vec{k}\cdot\vec{p}$ methods and deformation potential predicted type-I alignment when $x<0.4$,[27,28] there is growing evidence that strained SiGe/Si forms type-II alignment via exciton energy measurement and calculations.[29–33] However, regardless of the type of alignment, the magnitude is small and the impact of electron affinity on segregation is minimal. We linearly interpolated the value at $x=0.48$ that was provided by Ni *et al.*,[29] which was more conservative than that of Penn *et al.*[31]

Figure 3 shows a comparison between our calculations and experimental results for P segregation. The calculated segregation ratio predicts segregation out of strained SiGe, as

seen in experiments, but underestimates the extent of segregation. At least some of this difference may be due to issues related to the experiments. In particular, we can note that differences between the value of Christensen *et al.*[12] and our intrinsic value become larger as the Ge fraction increases. If partial relaxation had occurred as they reported, stress energy would be reduced and stronger segregation into Si would be expected. In addition, a Si capping layer on top of partially relaxed $Si_{1-x}Ge_x$ experiences lattice expansion, and the electron affinity increase due to conduction-band lowering[14,34] overwhelms smaller difference in the band gap in Eq. (10), and the prefactor in Eq. (10) is lowered. The Kobayashi *et al.*[35] result deviates substantially from the theoretical calculation, which can be attributed to partial lattice relaxation in such thick (160–400 nm) $Si_{0.75}Ge_{0.25}$ layers and slow chemical potential increase due to partial activation in the Si layer. Partial activation arises when N is near 2×10^{20} cm^{-3} (Ref. 36) and reduces the chemical potential with the fractional contribution of the electric potential energy of the ion [see Eq. (7)]. In the inset of Fig. 3, we also compared the As segregation ratio to the data of Hu *et al.*[5] Due to the small induced strain of As, stronger segregation than P is expected. The value extracted from experiment is lower than the calculated value, possibly due to ignoring the higher As diffusivity in strained $Si_{1-x}Ge_x$ (Ref. 13) than in Si.

In acceptor-doped semiconductors, the majority charge carriers are holes; thus, $Z=-1$. Combined with large stress effects, the result is B segregation into the $Si_{1-x}Ge_x$ layer. Figure 4 shows a comparison between our prediction and measured values for B segregation. Overall, the prediction appears quite good, with the calculations generally predicting slightly more segregation into the strained SiGe than observed experimentally. The largest difference is for the result of Fang *et al.*[8] with low B concentration ($C_B\sim3\times10^{17}$ cm^{-3} in Si region), which shows substantially less segregation than our calculation. This at least is partially due to the narrowness of the $Si_{1-x}Ge_x$ layer. In their experiment, the Debye length is about 11 nm but the half width of the $Si_{1-x}Ge_x$ layer is 15 nm, so the built-in potential is not fully developed. In B segregation, stress effects are dominant but the change in the band structure still has a significant effect.

In conclusion, we developed general expressions for segregation of dopants in strained semiconductor heterostructure. Based on this analysis, we calculated dopant segregation ratio at Si/strained-SiGe interface by considering band alignment, band-gap narrowing due to biaxial compressive stress, effective density of states, and stress energy as a function of Ge fraction and temperature. We find that stress is the dominant factor for B and changes in band-structure dominate for P and As. The predicted segregation shows good agreement with experimental measurement.

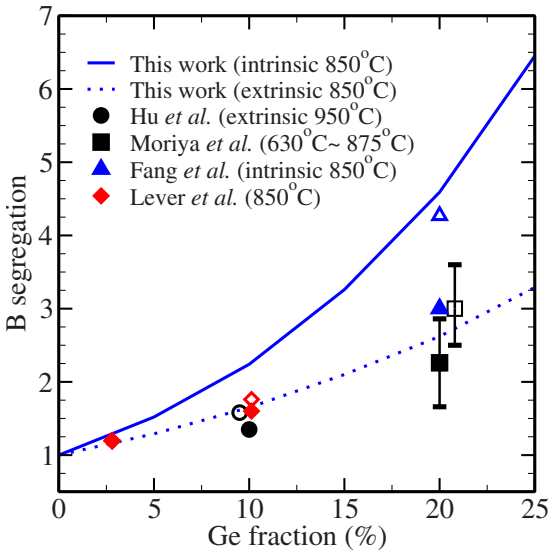

FIG. 4. (Color online) B segregation ratio at Si/strained-SiGe interface. Filled symbols represent measured values and open symbols represent theoretical values. At low Ge concentration (3% Ge), the Lever *et al.* (Ref. 6) data and predicted value overlap. The error bar with open square is for comparison with the Moriya *et al.* (Ref. 7) data at various temperatures. For better visibility, theoretical values corresponding to data of Moriya *et al.* (Ref. 7) and Hu (Refs. 1 and 2) are plotted with a small offset in Ge concentration.

This work was funded by the Semiconductor Research Corporation (SRC). DFT calculations were performed using computer hardware donated by Intel and AMD as well as under NSF Grant No. EIA-0101254.

[1] S. M. Hu, Phys. Rev. Lett. **63**, 2492 (1989).
[2] S. M. Hu, Phys. Rev. B **45**, 4498 (1992).
[3] C. Ahn, M. Diebel, and S. T. Dunham, J. Vac. Sci. Technol. B **24**, 700 (2006).
[4] P. Boguslawski, N. G. Szwacki, and J. Bernholc, Phys. Rev. Lett. **96**, 185501 (2006).
[5] S. M. Hu, D. C. Ahlgren, P. A. Ronsheim, and J. O. Chu, Phys. Rev. Lett. **67**, 1450 (1991).
[6] R. F. Lever, J. M. Bonar, and A. F. W. Willoughby, J. Appl. Phys. **83**, 1988 (1998).
[7] N. Moriya, L. C. Feldman, S. W. Downey, C. A. King, and A. B. Emerson, Phys. Rev. Lett. **75**, 1981 (1995).
[8] T. T. Fang, W. T. C. Fang, P. B. Griffin, and J. D. Plummer, Appl. Phys. Lett. **68**, 791 (1996).
[9] C. Ahn, Ph.D. thesis, University of Washington, 2007.
[10] C. Ahn and S. T. Dunham, J. Appl. Phys. **102**, 123709 (2007).
[11] C. Ahn, J. Song, and S. T. Dunham, *Transistor Scaling-Methods, Materials and Modeling*, MRS Symposia Proceedings No. 913 (Materials Research Society, Pittsburgh, 2006), p. 179.
[12] J. S. Christensen, H. H. Radamson, A. Yu. Kuznetsov, and G. G. Svensson, J. Appl. Phys. **94**, 6533 (2003).
[13] S. Uppal, J. M. Bonar, J. Zhang, and A. F. W. Willoughby, Mater. Sci. Eng., B **114-115**, 349 (2004).
[14] L. Yang, J. R. Watling, R. C. Wilkins, M. Borici, J. R. Barker, A. Asenov, and S. Roy, Semicond. Sci. Technol. **19**, 1174 (2004).
[15] M. V. Fischetti and S. E. Laux, J. Appl. Phys. **80**, 2234 (1996).

[16] M. A. Green, J. Appl. Phys. **67**, 2944 (1990).
[17] Y. Fu, S. C. Jain, M. Willander, and J. J. Loferski, J. Appl. Phys. **74**, 402 (1993).
[18] Y. Okada and Y. Tokumaru, J. Appl. Phys. **56**, 314 (1984).
[19] F. Schaffler, *Properties of Advanced Semiconductor Materials GaN, AlN, InN, BN, SiC, SiGe*, edited by M. E. Levinshtein, S. L. Rumyantsev, and M. S. Shur (Wiley, New York, 2001), pp. 149–188.
[20] S. P. Nikanorov, Yu. A. Burenkov, and A. V. Stepanov, Sov. Phys. Solid State **13**, 2516 (1971).
[21] G. Kresse and J. Hafner, Phys. Rev. B **47**, 558 (1993); G. Kresse and J. Furthmüller *ibid.* **54**, 11169 (1996).
[22] J. P. Perdew, J. A. Chevary, S. H. Vosko, K. A. Jackson, M. R. Pederson, D. J. Singh, and C. Fiolhais, Phys. Rev. B **46**, 6671 (1992).
[23] G. S. Cargill, J. Angilello, and K. L. Kavanagh, Phys. Rev. Lett. **61**, 1748 (1988).
[24] A. Fukuhara and Y. Takano, Acta Crystallogr., Sect. A: Cryst. Phys., Diffr., Theor. Gen. Crystallogr. **33**, 137 (1977).
[25] M. R. Sardela, Jr., H. H. Radamson, J. O. Ekberg, J.-E. Sundgren, and G. V. Hansson, Semicond. Sci. Technol. **9**, 1272 (1994).
[26] C. Ahn and S. T. Dunham, Appl. Phys. Lett. **93**, 022112 (2008).
[27] C. G. Van de Walle and R. M. Martin, Phys. Rev. B **34**, 5621 (1986).
[28] M. El Kurdi, S. Sauvage, G. Fishman, and P. Boucaud, Phys. Rev. B **73**, 195327 (2006).
[29] W.-X. Ni, J. Knall, and G. V. Hansson, Phys. Rev. B **36**, 7744 (1987).
[30] T. Baier, U. Mantz, K. Thonke, R. Sauer, F. Schäffler, and H.-J. Herzog, Phys. Rev. B **50**, 15191 (1994).
[31] C. Penn, F. Schäffler, G. Bauer, and S. Glutsch, Phys. Rev. B **59**, 13314 (1999).
[32] M. L. W. Thewalt, D. A. Harrison, C. F. Reinhart, J. A. Wolk, and H. Lafontaine, Phys. Rev. Lett. **79**, 269 (1997).
[33] H. H. Cheng, S. T. Yen, and R. J. Nicholas, Phys. Rev. B **62**, 4638 (2000).
[34] R. Arghavani, S. Solmi, A. Parisini, R. Angelucci, A. Armigliato, D. Nobili, and L. Moro, IEEE Trans. Electron Devices **54**, 362 (2007).
[35] S. Kobayashi, M. Iizuka, T. Aoki, and N. Mikoshiba, J. Appl. Phys. **86**, 5480 (1999).
[36] S. Solmi, A. Parisini, R. Angelucci, A. Armigliato, D. Nobili, and L. Moro, Phys. Rev. B **53**, 7836 (1996).